Responses to comments of Reviewer 3

Dear Reviewer 3:

We greatly appreciate your suggestions, and we hope our revisions have addressed your questions and made this manuscript better.

Sincerely,
Dr. Siming He

Comment 1. My general comment in that the results presented in manuscript are not discussed. Additionally, figure captions need to expand and explain the figure in a brief and simple way, so the reader doesn0t need to switch back to the tex to understand the figure.

Response.

(1) According to your suggestion, we have discussed the results.

Page 7, line 9 and 10

Page 9, line 16 and 17

Page 10, line 1 to 6

(2) According to your suggestion, we have modified the figure captions.

Page 6, line 2

Page 7, line 12

Page 9, line 6

Comment 2. I have read the first review of the manuscript, and I agree with the reviewer that it is essencial to show multi-frequency and phase data.

Response.

We added Phase(f) to the experiment on synthetic SSIP data record. Figures 1 and 2 show the relative error of Phase(f) are calculated and compared at the three main frequencies when the noise RMS ranges from 0 to 0.9.

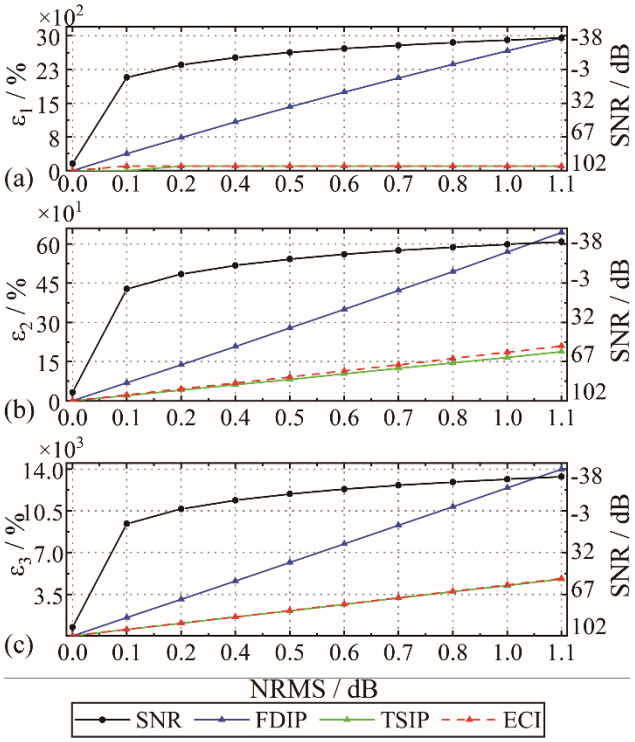

Figure 1. The effect of different degrees of Gaussian noise to the measures excitation signals in the phase-frequency characteristics. (a) SNR of the polluted potential signal. Complex resistivity relative error at (b) 80 Hz, (c) 160 Hz, (d) 320 Hz comparison using the three methods.

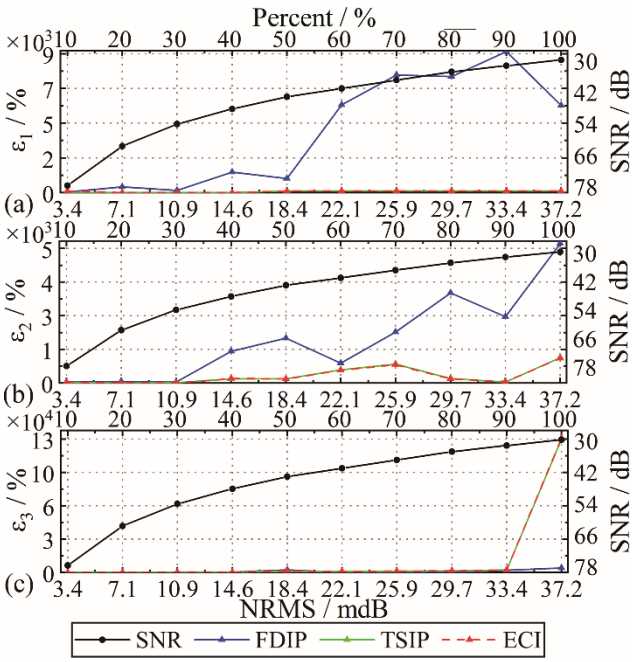

Figure 2. The effect of different levels of spike noises to the measured excitation signals. (a) SNR of the contaminated potential signal in the phase-frequency characteristics. Complex resistivity relative error at (b) 80 Hz, (c) 160 Hz, (d) 320 Hz comparison using the three methods.

From Figures 1 and 2, the results do not reflect the noise reduction performances of the three algorithms. Therefore, these results are not put into our manuscript. But |R(f)| and Phase(f) processed by three algorithms reflect their noise reduction performance well in the field

experiment, as shown in Figure 3. So |R(f)| and Phase(f) in the field experiment are added to our manuscript.

This information is added on Page 9, line 16 and 17, Page 10, line 1 to 5 and Figure 3.

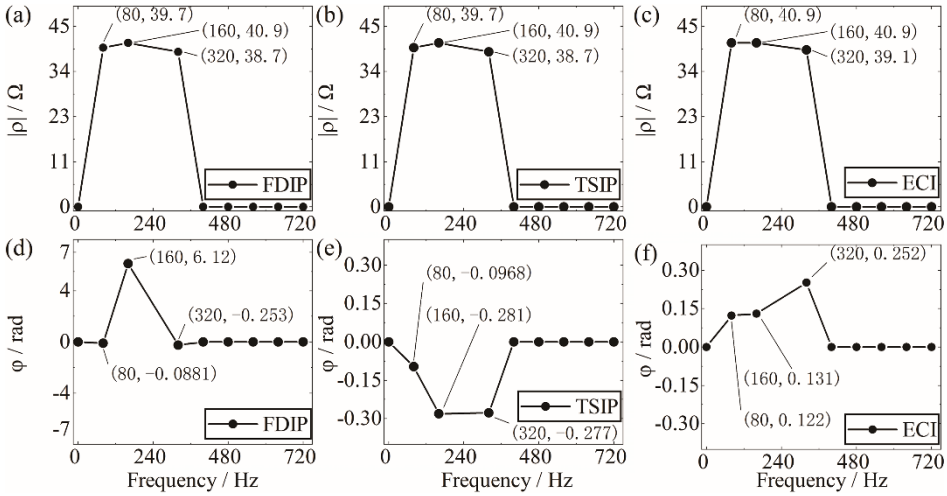

Figure 3. Complex resistivity spectrum calculated by the three algorithm (one period) in survey point No 21.

Comment 3. Page 7: "ECI algorithm still has superior denoising performance and holds smaller volatility of the relative error when the percentage of the outliers is more significant than 50% ." What do you mean by volatility here? This sentence is unclear.

Response.

By 'volatility' we were trying to say 'fluctuation', sorry for causing misunderstanding.

Page 6, line 8

Comment 4. What situations would the algortim fail? That is, what are the limitations? Please show the limitations in detail (simulation or measured data and discussion).

Response.

In a real environment, this model is contaminated by the environment interference and measuring instrument. It can be categorized into three types: the Gaussian random noise, the impulse interference, and the particular frequency disturbance (Wang and Li, 1986; Yan et al., 2016).

For our system, we assume the three noises are linearly overlapping on the three sensors, along with some weak influence of coupling effects. So, the noises in the three sensors are only different in amplitude. Hence,

$$n_1(t) = B_1 g(t) + C_1 p(t) + D_1 s(t) \tag{1}$$

$$n_2(t) = B_2 g(t) + C_2 p(t) + D_2 s(t) \tag{2}$$

$$n_3(t) = B_3 g(t) + C_3 p(t) + D_3 s(t) \tag{3}$$

where $n_k(t)$ is the noise in sensor Y_k, $k = 1, 2, 3$, respectively. $g(t)$, $p(t)$ and $s(t)$ are

separately Gaussian random noise, impulsive noise and particular frequency interference. B_k, C_k and D_k are the amplitudes of $g(t)$, $p(t)$ and $s(t)$, $k = 1, 2, 3$, respectively.

According to the properties of the correlation function, the cross-correlation results of the three kind of noise is as below:

A. For the Gaussian random noise, when $-NT \le \tau \le NT$ and $\tau \ne 0$, $R_{gg}(\tau)$ is shown in Figure 4.

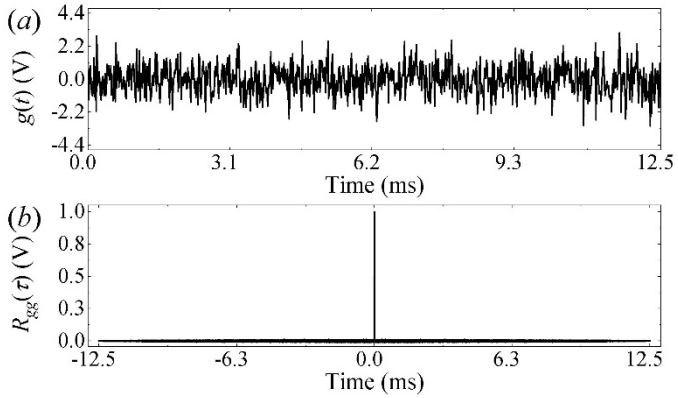

Figure 4. Waveform and autocorrelation for the Gaussian random noise $g(t)$. (a) its time domain waveform. (b) its autocorrelation $R_{gg}(\tau)$.

B. For the impulsive noise, when $-NT \le \tau \le NT$ and $\tau \ne 0$, it is considered that $R_{pp}(0) \gg R_{pp}(\tau)$, as shown in Figure 5.

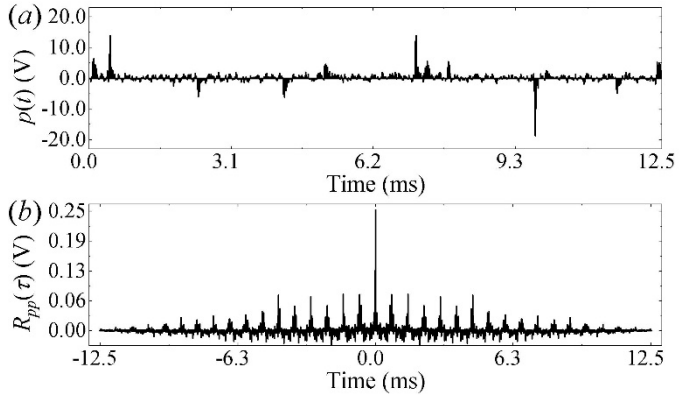

Figure 5. Waveform and autocorrelation for the impulsive noise $p(t)$. (a) its time domain waveform containing 20% of the outliers. (b) its autocorrelation $R_{pp}(\tau)$.

C. For the particular frequency disturbance, its autocorrelation has the same frequency with it, but when it is less effective for the transmitter output signal $u_{ab}(t)$ than that of the $u_{mn}(t)$ and $i(t)$,

$D_1D_2R_{ss}(\tau)$ and $D_1D_3R_{ss}(\tau)$ can be effectively suppressed, as shown in Figure 6.

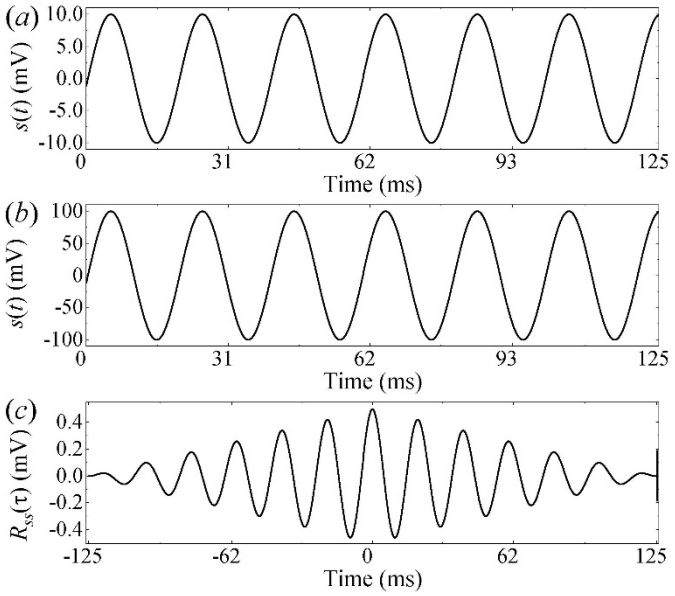

Figure 6. Waveform and autocorrelation for the particular frequency interference $s(t)$. The power-line interference (a) at $D_1 = 0.01$, (b) at $D_2 = 1$. (c) their cross-correlation $D_1D_2R_{ss}(\tau)$.

Based on the analysis above, it can be concluded that the influences of Gaussian random and impulsive noises are more effectively suppressed, while the particular frequency disturbance is attenuated to some degree when the noise is in lower intensity. Therefore, the proposed method has more value on denoising for Gaussian and impulsive random noises.

Page 10, line 15 and 16

References

Wang, F.S., and Li, T., 1986, Industry of stray current resistivity observation and avoid interference distance: Northeastern Seismological Research, 2, 44–48. doi:10.13693/j.cnki.cn21-1573.1986.02.006

Yan, T. J., Wang, S. Q., Mang, Y. X., and Luo, X. Z., 2016, Influence of human interference on application of electrical prospect-ing and corresponding anti–interference measures , Mineral Exploration, 7, 634–639. doi:10.3969/j.issn.1674-7801.2016.04.016

Comment 5. Phase (or quadradture component) results must be presented and discussed, oth-erwise we are not looking at the IP effects.

Response.

(1) The phase results for the inversion results given by Res2DInv software is shown as Figure 7. As we can see, this figure shows chaos information from the phase shift between $i(t)$ and $u(t)$ of the three methods. This is because the loss layer surrounding the shelter is very weak polarized, so the phase shift is very small, which cause the result easily contaminated by some random factors. Therefore, we have not figured out how to extract meaningful information out of the phase results, but it is possible that with proper strong-polarized experiment field there could be different results. We are eager to explore that in our next experiment plan.

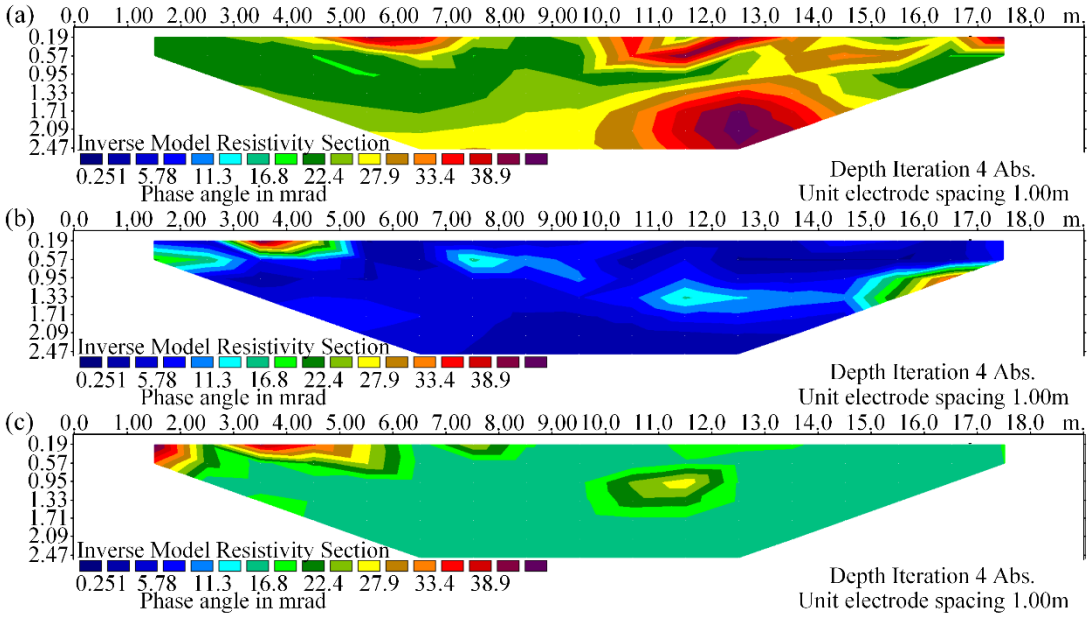

Figure 7. Inverted phase sections of the two high resistivity anomalies at 80Hz with using (a) the FDIP method, (b) the TSIP algorithm, and (c) the ECI algorithm.

(2) We added phase results to field experiment and not to simulation as we explained in Response 2.